*Work supported by Fonds zur Förderung der Wissenschaft, Austria.

[1]E.g., J. G. Ruch and G. Kino, Appl. Phys. Letters 10, 40 (1967).
[2]A. Zylberstejn and J. B. Gunn, Phys. Rev. 157, 668 (1967).
[3]G. A. Acket, Phys. Letters 25A, 374 (1967).
[4]H. Heinrich and W. Jantsch, Phys. Status Solidi 38, 225 (1970).
[5]H. Heinrich, K. Lischka, and M. Kriechbaum, Phys. Rev. B 2, 2009 (1970).
[6]M. A. Omar, Phys. Rev. 171, 925 (1968).
[7]H. K. Kar and M. N. Mukherjee, Phys. Letters 30A, 355 (1969).
[8]H. Heinrich, Phys. Letters 32A, 331 (1970).
[9]J. S. Craig, R. F. Gribble, and A. A. Dougal, Rev. Sci. Instr. 35, 1501 (1964).
[10]R. A. Smith, *Semiconductors* (Cambridge U. P., Cambridge, England, 1964).
[11]G. Bordure and F. Gustavino, Compt. Rend. 267, 860 (1968).
[12]C. Y. Liang, J. Appl. Phys. 39, 3866 (1968).
[13]*American Institute of Physics Handbook*, edited by D. E. Gray (McGraw-Hill, New York, 1963).
[14]H. Piller, J. Appl. Phys. 37, 763 (1966).
[15]F. R. Kessler, Phys. Status Solidi 5, 3 (1964).
[16]M. Balkansky and E. Amzallag, Phys. Status Solidi 30, 407 (1968).
[17]V. E. Wood, J. Appl. Phys. 40, 3740 (1969).
[18]I. P. Ipatova, P. E. Kazarinov, and A. V. Shubashiev, Fiz. Tverd. Tela 7, 2129 (1965) [Soviet Phys. Solid State 7, 1714 (1966)].
[19]H. Piller, J. Phys. Chem. Solids 24, 425 (1963).
[20]E. O. Kane, J. Phys. Chem. Solids 1, 249 (1957).
[21]H. Piller, in *Proceedings of the International Conference on the Physics of Semiconductors, Moscow*, 1968 (Nauka Publishing House, Leningrad, 1968), p. 353.

PHYSICAL REVIEW B VOLUME 3, NUMBER 2 15 JANUARY 1971

High-Field Transport in the Three-Valley Conduction Band of Gallium Antimonide*

W. Jantsch and H. Heinrich
Institut für Angewandte Physik der Universität, A-1090 *Vienna, Austria*
and Ludwig-Boltzmann Institut für Festkörperphysik, Vienna, Austria

(Received 27 July 1970)

The j-E characteristics of Te-doped GaSb have been measured up to a field strength of 18 kV/cm at 300 °K and up to 7.5 kV/cm at 77 °K. Results for the longitudinal magnetoresistance and the Hall constant at 300 and 77 °K up to a field strength of about 7 kV/cm are given. Avalanche breakdown was observed at a field strength above 7 kV/cm, and the electron-hole pair generation rate at 300 °K was determined. Calculations based on a three-band model are compared with the measurements. For high-field strengths the influence of the highest X_1 minimum has to be taken into account to obtain agreement between experimental and calculated results. Attempts have been made at an experimental realization of the negative differential resistance (NDR) predicated by Zaitsev and Zvezdin due to virtual states below the L_1 minimum. The effect, although observable, has been found to be not sufficient to produce NDR.

I. INTRODUCTION

In a recent paper[1] we reported measurements of the electrical conductivity and the longitudinal magnetoresistance of GaSb at high electric fields. For calculation, a two-band model was used, in which we considered carrier transfer from the lowest conduction-band minimum (Γ_1) at the center of the Brillouin zone to the four minima (L_1) along the $\langle 111 \rangle$ directions in k space lying 0.1 eV above the Γ_1 minimum.[2] We now want to discuss a more detailed investigation of high-field galvanomagnetic properties of GaSb, and we present calculations which take into account the third type (X_1) of conduction-band minima, lying at the zone boundaries along the $\langle 100 \rangle$ directions, 0.315 eV above the Γ_1 minimum.[3] Hilsum and Rees[4] have considered the three-valley semiconductors for high-efficiency Gunn devices, and a Gunn effect has been reported for $Ga_xIn_{1-x}Sb$ alloys.[5] Therefore, it appears to be of interest to study the high-field behavior of the GaSb component of this system in connection with the proposed three-valley effect.

It is well known (see Butcher and Fawcett[6]) that according to a simple criterion no negative differential resistance (NDR) will be obtained when the energy separation of the lowest two sets of minima is less or comparable to $4kT$. This is obviously fulfilled for GaSb at 300 °K, and no NDR has been observed because of the thermal population of the L_1 minima. This offers the interesting possibility of studying electron transfer without experimental

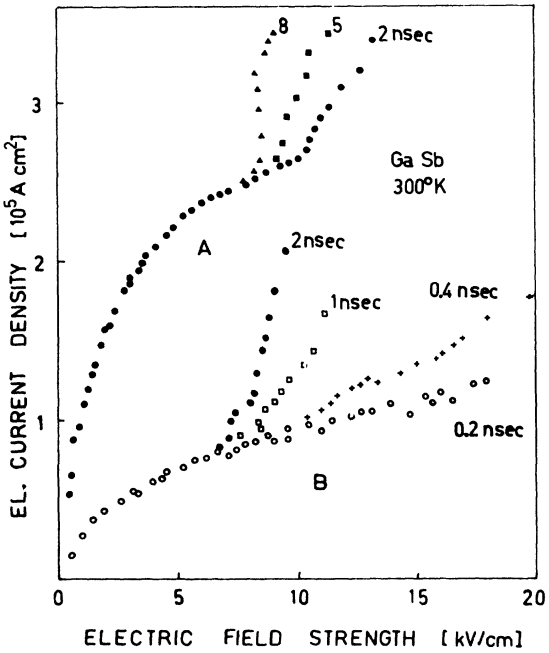

FIG. 1. j-E characteristics of n-type GaSb at 300 °K; the upper curve for a carrier concentration of 3×10^{17} e per/cm^3, the lower for 6.8×10^{16} e/cm^{-3}. Points for different times after application of the dc pulse are given.

difficulties arising from high-field domains and instabilities. At 77 °K, where the energy separation between L_1 and Γ_1 is greater than $4kT$, surprisingly no NDR or associated effects are observed. In the following we want to report experimental results for the j-E characteristic, the Hall constant, the longitudinal magnetoresistance, and the generation rate during avalanche breakdown as a function of applied electric field. The experimental results will be compared with calculations based on a three-band model, similar to the two-band calculation of Chynoweth and McCumber[7] and of Omar, [8] respectively. Finally, we will report careful investigations of the j-E characteristics at 77 °K at low electric fields for which a strong NDR due to electron capture by quasidiscrete levels of shallow donor impurities has been predicted by Zaitsev and Zvezdin. [9] We will show that this effect occurs in the predicted range of the electric fields although its magnitude is not sufficient for producing a NDR.

II. EXPERIMENTAL

Samples were cut from Te-doped material, such that the main axis was within (111) planes. Carrier concentration and mobilities were determined by making conductivity and Hall measurements and by taking into account two-band conduction together with the known value of the mobility ratio[2] $\mu_0/\mu_1 = 5.6$, where μ_0 and μ_1 are the mobilities in the Γ_1 and L_1 valleys, respectively. Contacts were prepared by alloying Sn plus 1% Sb to the end faces of the samples.

TABLE I. Carrier concentrations and mobilities of the materials under investigation as obtained from the two-band analysis of Hall and conductivity measurements.

n (cm^{-3})	n_0 (cm^{-3})	n_1 (cm^{-3})	μ_0 (cm^2/V sec)	μ_1 (cm^2/V sec)
6.8×10^{16}	3.05×10^{16}	3.76×10^{16}	3700	660
1.5×10^{17}	8.5×10^{16}	6.4×10^{16}	5000	890
3.5×10^{17}	1.45×10^{17}	2.05×10^{17}	4900	880

The j-E characteristics obtained at 300 °K are shown in Fig. 1, branch A, for a total electron concentration of 3.5×10^{17} e/cm^{-3}, and branch B, for 6.8×10^{16} e/cm^{-3}. Hall mobilities and electron concentrations are given in Table I. The observed decrease of mobility will be shown to be due to the electron transfer to the higher conduction-band minima. Avalanche breakdown is observed above 7 kV/cm for the pure samples and above 8.5 kV/cm for the less pure material. Values for different times t, after application of the electric field, are given in Fig. 1. For electric fields below avalanche breakdown, the j-E characteristic is time independent. The experimental points for $t \geq 1$ nsec were ob-

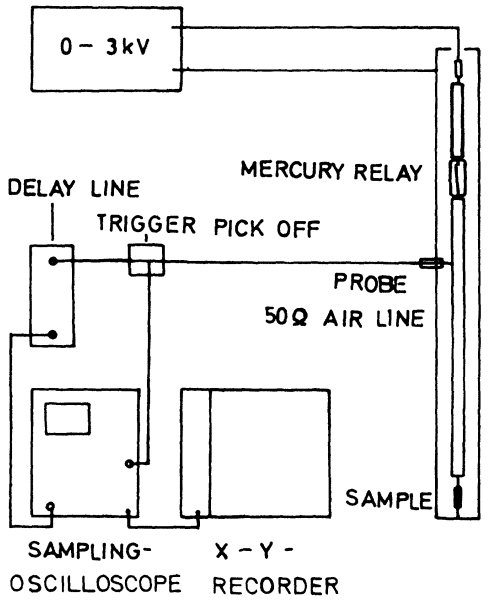

FIG. 2. Schematic diagram of the experimental arrangement used for the measurements 0.2 and 0.4 nsec after application of the dc pulse. Pulses are generated by discharging the coaxial line through a mercury-wetted relay which is operated by an electromagnet, 50 times per sec. The pulse is transmitted to the sample by a 50-Ω line. Both incoming and reflected pulses are picked up by a low-rise-time sampling probe, observed on a sampling oscilloscope, and plotted by an X-Y recorder.

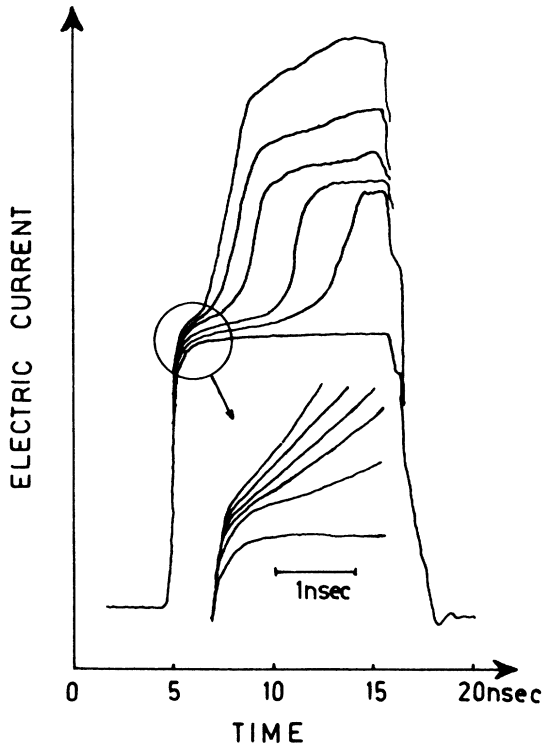

FIG. 3. Current pulses obtained on a sample with 6.8 $\times 10^{16}$ e/cm^3 at field strengths above the avalanche-threshold field strength. For low carrier generation and short time after application of the 10-nsec dc pulse, the current rises exponentially with time and saturates at high values of the carrier multiplication owing to the increasing recombination rate.

tained by observing the voltage drop between potential probes along the samples. The current was detected by the voltage drop on a resistor in series with the sample. The total pulse length was 10 nsec. Voltage and current pulses were observed on a X-Y recorder connected to a sampling oscilloscope. The points obtained 0.4 and 0.2 nsec after application of the electric field were measured using an experimental arrangement reported in detail recently.[10] It is shown schematically in Fig. 2. This method is based on a comparison of incident pulse and the pulse reflected from the sample, from which the j-E characteristic is obtained.

In order to obtain information about the generation rate during avalanche breakdown, current pulses were recorded at nearly constant voltage, as shown in Fig. 3. For low carrier generation and short periods after application of the dc voltage, the pulses rise exponentially with time and saturate at high values of the carrier multiplication because of the increasing influence of recombinations. According to a method reported by McGroddy and Nathan,[11] the generation rate g can be obtained by measuring dj/dt for short times after application of the field

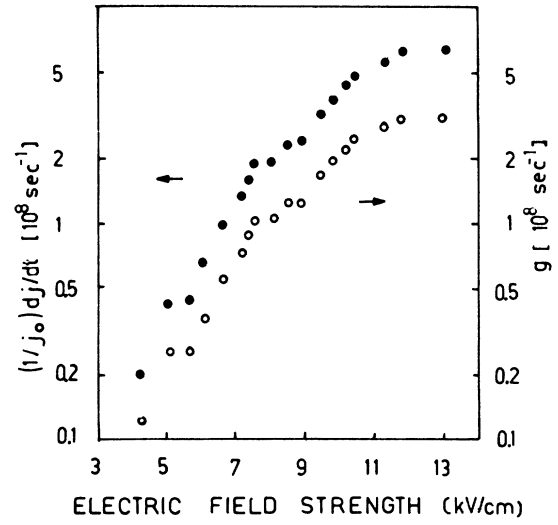

FIG. 4. Values (full dots) $(1/j_0)$ dj/dt obtained by evaluating the pulses of Fig. 3. The electron-hole pair generation rate g is obtained from $(1/j_0)$ dj/dt, taking into account the contribution of the generated holes to the conductivity. Values of g (E) are given also (circles).

where recombination is still negligible.

Measurements of $(1/j_0)$ dj/dt are plotted in Fig. 4. j_0 is the current just after application of the dc pulse and was determined from the j-E characteristic obtained 0.2 nsec after application of the pulse.

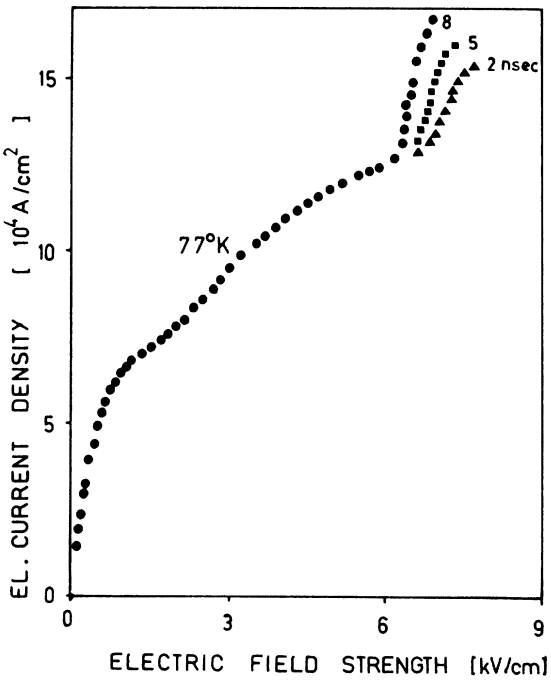

FIG. 5. j-E characteristic of n-type GaSb with 6.8 $\times 10^{16}$ e/cm^3 at 77 °K. Points for different times after application of the dc pulses are given.

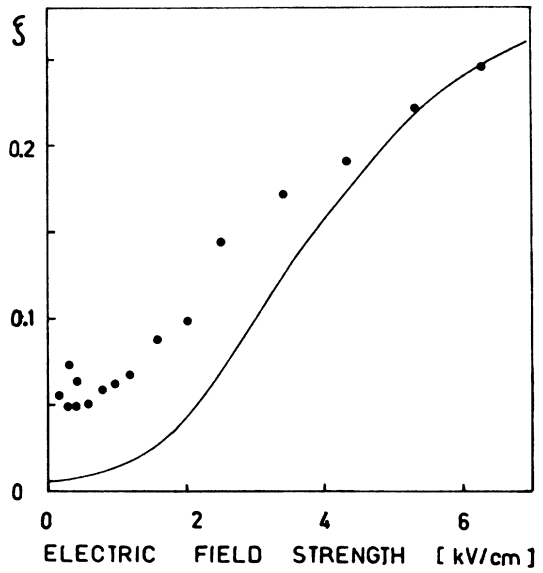

FIG. 6. Longitudinal magnetoresistance coefficient ζ in n-type GaSb with 6.8×10^{16} e/cm^{-3} at 300 °K. The dots are measured; the solid line is calculated.

At this time carrier multiplication was assumed to be still negligible. In contrast to InSb the influence of the generated holes on the conductivity has to be taken into account in order to obtain the generation rate for electron-hole pairs. A simple calculation gives

$$\frac{1}{n_0}\frac{dn}{dt}=\frac{1}{1+\mu_p/\mu_n}\,\frac{1}{j_0}\frac{dj}{dt}\,,$$

where μ_n is a mobility averaged over the Γ_1, L_1, and X_1 valleys determined from j_0; μ_p was assumed to be constant. Its value was taken as $\mu_p = 800$ cm^2/V sec, which was obtained from[12] $\mu_0/\mu_p = -4.6$, μ_0 being the mobility in the Γ_1 valley. The results for g are also given in Fig. 4.

In Fig. 5, the j-E characteristic for the 6.8×10^{16}-cm^{-3} material at 77 °K is given. Avalanche breakdown is observed at field strengths above 6.5 kV/cm.

As mentioned above, one would expect to observe an NDR at 77 °K. Therefore, this point has been investigated carefully since the formation of space charge could possibly obscure the NDR. However, a linear potential drop between the contacts has been observed up to the highest field strengths by probing the potential along the sample with high-impedance probes. This rules out any space-charge accumulation, and we consider the observed j-E characteristics to be a bulk property of the material.

Figures 6 and 7 show experimental results for the longitudinal magnetoresistance $\zeta = (\Delta\rho/\rho_0)\times(1/\mu B)^2$ as a function of the electric field. ζ grow strongly with increasing field strength. This is assumed to be due to the increasing occupation of the Ge-like L_1 minima by electrons as they become hot, since only these electrons contribute to ζ, while the contribution to the longitudinal magnetoresistance by the spherical Γ_1 minimum vanishes.

The Hall constant measured as a function of electric field is plotted in Fig. 8 for 300 °K and 77 °K, respectively. The measurements were performed with pulses of 10 nsec duration at different times after application of the pulses. The samples had side arms to minimize contact effects. The Hall constant exhibits a maximum which is typical for two-band conduction. At field strength above 7 kV/cm a time dependence of the Hall constant is observed, which is attributed to the avalanche breakdown.

III. DISCUSSION

We have performed calculations for the conductivity, the Hall constant, and the magnetoresistance based on a simple model deduced from the theories by Chynoweth and McCumber[7] and by Omar.[8] For simplicity the following assumptions are made: (i) There is Maxwellian energy distribution in the three types of valleys with common electron temperature T_e; (ii) there is an energy relaxation time τ_ϵ; and (iii) the electron mobilities μ_0, μ_1, μ_2 in the three types of valleys are independent of T_e. Although some of these assumptions are very crude, the application of this model may be justified by the direct physical insight offered and the excellent agreement with the experimental data. Also recent experimental investigations of the infrared Faraday rotation revealed that the calculated electron transfer is in good agreement with the experimental values.[13] The average drift velocity $\langle v_d\rangle$ is given

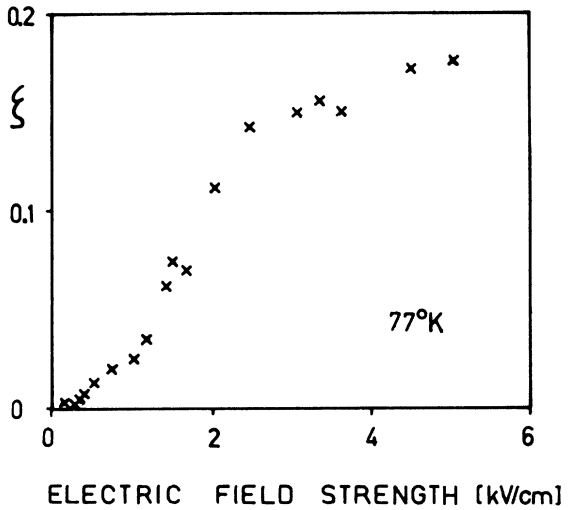

FIG. 7. Longitudinal magnetoresistance coefficient ζ in n-type GaSb with 6.8×10^{16} e/cm^{-3} at 77 °K.

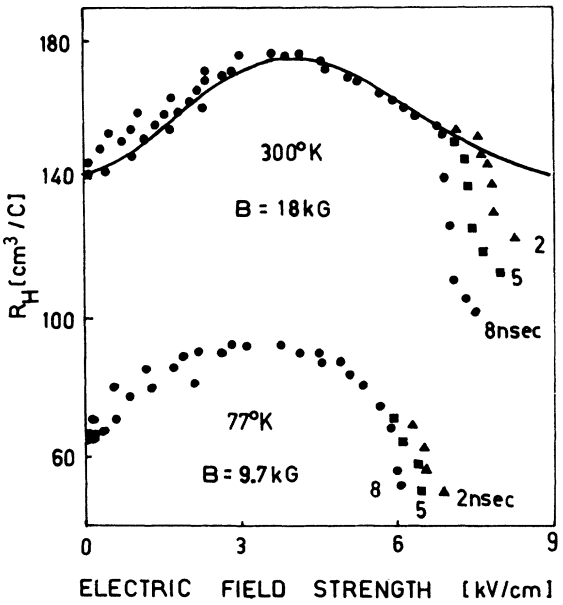

FIG. 8. Hall constant as a function of electric field in GaSb at 300 and 77 °K. Values for different times after application of the electric field are given. The solid line is calculated for 300 °K.

by

$$\langle v_d \rangle = \frac{n_0 \mu_0 + n_1 \mu_1 + n_2 \mu_2}{n_0 + n_1 + n_2} E, \tag{1}$$

where E is the electric field strength and the n_i are the electron concentrations in the Γ_1, L_1, and X_1 minima, respectively, given by

$$n_i = 4\pi M_i \left(\frac{2m_i^* k T_e}{h^2}\right)^{3/2} \mathfrak{F}_{1/2}\left(\frac{\epsilon_F - \Delta_i}{kT_e}\right), \quad i = 0, 1, 2 \tag{2}$$

where ϵ_F is the Fermi level. $i = 0$ stands for the Γ_1 minimum, $i = 1$ for the L_1, and $i = 2$ for the X_1 minima. m_i^* is the density-of-states effective mass, Δ_i is the separation from the Γ_1 minimum, and M_i is the multiplicity of the valleys of one type. $\mathfrak{F}_{1/2}$ are Fermi integrals. The total electron concentration n was assumed to be constant:

$$n = n_0 + n_1 + n_2 . \tag{3}$$

E and $\langle v_d \rangle$ are related by the energy balance equation

$$eE\langle v_d \rangle = [\langle \epsilon(T_e) \rangle - \langle \epsilon(T_l) \rangle]/\tau_\epsilon , \tag{4}$$

where T_l is the lattice temperature, and

$$\langle \epsilon(T_i) \rangle = \tfrac{3}{2} kT_i + \frac{\alpha_1 \Delta_1 e^{-\Delta_1/kT_i} + \alpha_2 \Delta_2 e^{-\Delta_2/kT_i}}{1 + \alpha_1 e^{-\Delta_1/kT_i} + \alpha_2 e^{-\Delta_2/kT_i}} , \tag{5}$$

where T_i is T_e or T_l, and α_1 and α_2 are the ratios of the densities of states in the upper valleys to the density of states at the Γ_1 minimum. From Eqs. (1)–(5), $\langle v_d \rangle$ is obtained as a function of the electric field strength E. All constants but α_2 and τ_ϵ are known from previous papers (see Table II). α_2, the ratio of the density of states at the X_1 minima and the density of states at the Γ_1 minimum, was assumed to be equal to α_1. In Fig. 9 results for n_0, n_1, n_2 as a function of the electric field are given.

Assuming polar optical-mode scattering to be the dominant mechanism for the energy loss, we have calculated τ_ϵ as a function of T_e. τ_ϵ is obtained from the expression for $d\epsilon/dt$, as given by Conwell, [16]

$$\left(\frac{d\epsilon}{dt}\right)_{po} = -\left(\frac{2k\Theta_D}{\pi}\right)^{1/2} \frac{m^{1/2} e^2 \hbar \omega_l}{\hbar^2} \left(\frac{1}{\kappa_\infty} - \frac{1}{\kappa_0}\right) \times \frac{e^{x_0 - x_e} - 1}{e^{x_0} - 1} x_e^{1/2} e^{x_e/2} K_0(x_e/2) , \tag{6}$$

where Θ_D is the Debye temperature, ω_l is the longitudinal optical-mode frequency, κ_0 and κ_∞ are the statical and the optical dielectric constants, respectively, and x_0 and x_e represent $\hbar\omega_l/kT_l$ and $\hbar\omega_l/kT_e$, respectively. $m^{1/2}$, the square root of the effective mass, was averaged over the three types of valleys. Although no energy relaxation time in the rigorous meaning does exist for polar optical-mode scattering, the quantity τ_ϵ defined by

$$-\frac{d\epsilon}{dt} = \frac{\langle \epsilon(T_e) \rangle - \langle \epsilon(T_l) \rangle}{\tau_\epsilon}$$

may be used in (4) to calculate the energy gain. τ_ϵ as a function of T_e has been plotted in Fig. 10 and has been found to be nearly energy independent over a wide range of T_e. Therefore, we used for the numerical calculations at 300 °K an energy-independent value of $\tau_\epsilon = 4 \times 10^{-12}$ sec which is close to those calculated and which gives the best agreement with our experimental data.

In Fig. 11 the experimental points obtained 0.2

TABLE II. Constants used in the numerical calculation.

$m_0 = 0.05\ m_0$	Effective mass in Γ_1 [a]
$m_{1t} = 0.143\ m_0$	Transverse effective mass in L_1 [a]
$K = 8.6$	Anisotropy coefficient in L_1 [a]
$\alpha_1 = \alpha_2 = 56.5$	Effective density-of-states ratio [b]
$\Delta_1 = 0.1$ eV	Energy separation between Γ_1 and L_1 [a]
$\Delta_2 = 0.315$ eV	Energy separation between Γ_1 and X_1 [c]
$\tau_\epsilon = 4 \times 10^{-12}$ sec	Energy relaxation time [b]
$b_1 = 5.6$	Mobility ratio μ_0/μ_1 [a]
$b_2 = 32$	Mobility ratio μ_0/μ_2 [c]
$\Theta_D = 265$ °K	Debye temperature [d]
$\kappa_0 = 15.2$	Static dielectric constant [e]
$\kappa_\infty = 16.5$	Optical dielectric constant [e]

[a] Reference 2.
[b] See text.
[c] Reference 3.
[d] Reference 14.
[e] Reference 15.

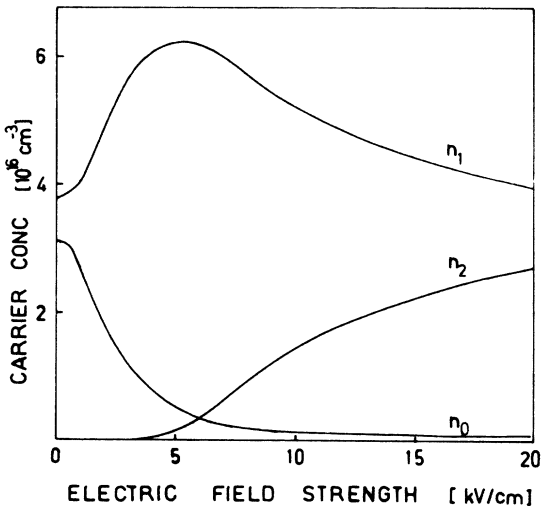

FIG. 9. Calculated values for n_0, n_1, n_2 as a function of the electric field, for a total carrier concentration of $n = 6.8 \times 10^{16}$ cm^{-3}.

nsec after application of the pulse are compared with results from the calculations (solid curves). The experimental points obtained at 0.2 nsec are believed to represent the values without appreciable carrier generation since the same curves have been obtained for 0.25 nsec. In calculating the upper curve, the influence of the X_1 minima was neglected. For the lower curve all three types of minima were taken into account. Up to fields of 7 kV/cm the influence of the X_1 minima is negligible.

In Fig. 6 the calculated results for ξ are given (solid curve). The calculations were performed in the same way as reported recently.[1] The discrepancy between experimental and theoretical results at zero electric field may be due to a small disalignment of the sample axis in the longitudinal magnetic field. This should cause a contribution to ξ by the strong transverse magnetoresistance of electrons in Γ_1. This discrepancy apparently disappears at high electric fields where Γ_1 is depleted from electrons.

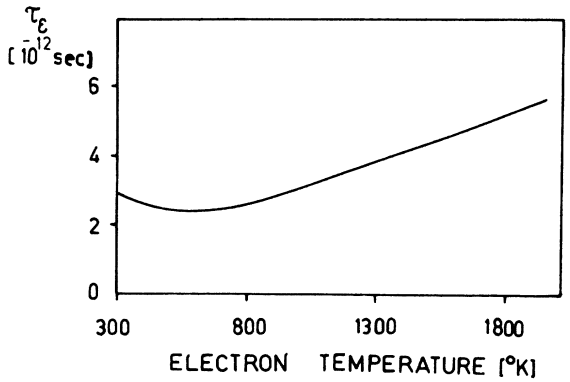

FIG. 10. Energy relaxation time τ_ϵ as a function of electron temperature T_e at 300 °K calculated for polar optical-mode scattering. The constants used are listed in Table II.

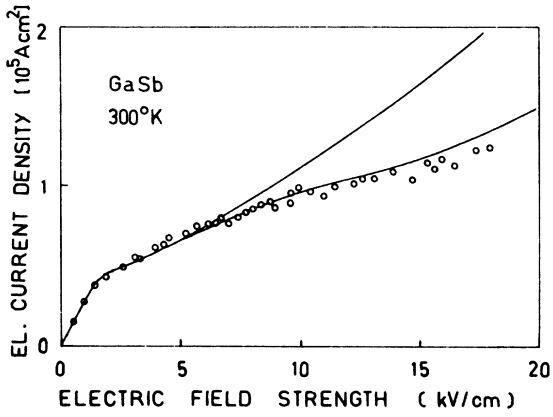

FIG. 11. Calculated j-E characteristic for 300 °K. For the upper curve only the Γ_1 and L_1 minima were taken into account, for the lower one the X_1 valleys were also considered. The experimental points are taken from Fig. 1.

In order to get quantitative theoretical results for the Hall constant, the usual formula for two-band conduction was used:

$$R_H = -\frac{1}{e}\,\frac{n_0\mu_0^2 + n_1\mu_1^2 + \mu_0^2\mu_1^2(n_0+n_1)B^2}{(n_0\mu_0 + n_1\mu_1)^2 + \mu_0^2\mu_1^2(n_0+n_1)^2B^2}\,. \qquad (7)$$

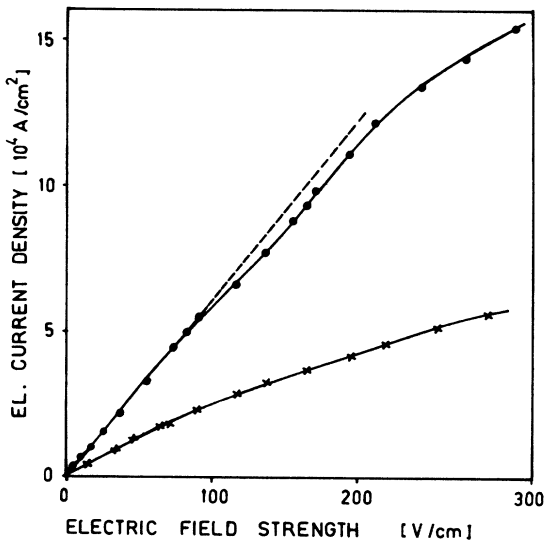

FIG. 12. j-E characteristics of Te-doped GaSb at 77 °K; upper points for a carrier concentration of 3.5×10^{17} cm^{-3}, lower for 1.5×10^{17} cm^{-3}. For the more highly doped material, in the range of 100–200 V/cm, an abnormal variation of σ is observed which is believed to be due to the effect predicted by Zaitsev and Zverzdin (Ref. 9).

The solid curve in Fig. 5 is calculated by inserting the calculated values of n_0 and n_1 into Eq. (7).

Also, we tried to make calculations for $T_l = 77\,^\circ$K, but the results for the j-E characteristics exhibit a NDR in contrast to our measurements. Obviously, the assumptions made in this calculation are not realistic for 77 °K such as a constant energy relaxation time which is applicable only at high temperature.

IV. INFLUENCE OF QUASIDISCRETE DONOR LEVELS

In Fig. 12 the j-E characteristics at 77 °K at moderate fields are given for electron concentrations of 3.5×10^{17} and 1×10^{17} e/cm^{-3}. These measurements were performed with pulses of 200 nsec duration. In a recent paper, negative differential conductivity was predicted for Te-doped material.[9] It was assumed that shallow donor impurities have quasidiscrete levels associated with higher conduction-band minima. When the electrons are heated by an electric field they gain energy and may be captured by levels connected with the L_1 minima. This reduction of the electron density could yield a NDR. Actually no NDR was observed and space-charge accumulation has been excluded by the same arguments as reported above. However, the measurements at the higher doped material show a small deviation from the Ohmic line (dashed in Fig. 12) which may be due to this effect. This is in agreement with the results of Ref. 9, where an effect of increasing magnitude with increasing donor concentration is predicted. Moreover, the effect is observed within the postulated range of electric fields of about 70–180 V/cm.

V. CONCLUSION

We have reported measurements of the j-E characteristics, the magnetoresistance, and the Hall effect as a function of the electric field. It has been shown that an interpretation of the experimental results obtained at 300 °K is possible in terms of a three-band conduction mechanism, and that carrier transfer by the electric field has to be taken into account. Influence of the third conduction-band minimum has been found to be important above 7 kV/cm for measurements obtained at short periods after the application of the dc voltage to the sample, when avalanche breakdown is negligible. A small deviation of the j-E characteristics is observed at 77 °K and at low electric fields which may be attributed to the influence of quasidiscrete levels associated with the L_1 conduction bands, as has been predicted by Zaitsev and Zvezdin. In the absence of a theoretical treatment based on the basic transport properties, no explanation can be given so far for the results obtained at 77 °K.

ACKNOWLEDGMENT

The authors want to express their appreciation to Professor K. Seeger for his stimulating interest in our work.

---

*Work supported by Fonds zur Förderung der Wissenschaftlichen Forschung, Austria.

[1]H. Heinrich and W. Jantsch, Phys. Status Solidi 38, 225 (1970).

[2]C. Y. Liang, J. Appl. Phys. 39, 3866 (1968).

[3]B. B. Kosicki, A. Jayaraman, and W. Paul, Phys. Rev. 172, 764 (1968).

[4]C. Hilsum and H. D. Rees, Electron. Letters 6, 277 (1970).

[5]J. C. McGroddy, M. R. Lorenz, and T. S. Plaskett, Solid State Commun. 7, 901 (1969).

[6]P. N. Butcher and W. Fawcett, Proc. Phys. Soc. (London) 86, 1205 (1965).

[7]A. G. Chynoweth and D. E. McCumber, IEEE Trans. Electron. Devices 13, 4 (1966).

[8]M. A. Omar, Phys. Rev. 171, 925 (1968).

[9]A. N. Zaitsev and A. K. Zvezdin, Zh. Eksperim. i Teor. Fiz. Pis'ma v Redaktsiyu 10, 8 (1969) [Soviet Phys. JETP Letters 10, 4 (1969)].

[10]W. Jantsch and H. Heinrich, Rev. Sci. Instr. 41, 228 (1970).

[11]J. C. McGroddy and M. I. Nathan, J. Phys. Soc. Japan Suppl. 21, 437 (1966).

[12]J. C. Woolley and C. M. Gillett, J. Phys. Chem. Solids 17, 34 (1960).

[13]H. Heinrich, Phys. Letters 32A, 331 (1970).

[14]R. L. Micher, Phys. Rev. Letters 4, 57 (1960); Phys. Rev. 125, 1537 (1962).

[15]*American Institute of Physics Handbook*, edited by D. E. Gray (McGraw-Hill, New York, 1963), pp. 9–49.

[16]E. M. Conwell, *High Field Transport in Semiconductors* (Academic, New York, 1967), p. 159.